ORIGINAL PAPER

Impact of Gas Adsorption Induced Coal Matrix Damage on the Evolution of Coal Permeability

W. C. Zhu · C. H. Wei · J. Liu · T. Xu · D. Elsworth

Abstract It has been widely reported that coal permeability can change from reduction to enhancement due to gas adsorption even under the constant effective stress condition, which is apparently inconsistent with the classic theoretical solutions. This study addresses this inconsistency through explicit simulations of the dynamic interactions between coal matrix swelling/shrinking induced damage and fracture aperture alteration, and translations of these interactions to permeability evolution under the constant effective stress condition. We develop a coupled coal–gas interaction model that incorporates the material heterogeneity and damage evolution of coal, which allows us to couple the progressive development of damage zone with gas adsorption processes within the coal matrix. For the case of constant effective stress, coal permeability changes from reduction to enhancement while the damage zone within the coal matrix develops from the fracture wall to further inside the matrix. As the peak Langmuir strain is approached, the decrease of permeability halts and permeability increases with pressure. The transition of permeability reduction to permeability enhancement during gas adsorption, which may be closely related to the damage zone development in coal matrix, is controlled by coal heterogeneity, external boundary condition, and adsorption-induced swelling.

1 Introduction

Coal is a typical dual-porosity/permeability system containing porous matrix surrounded by fractures (Seidle et al. 1992). These natural fractures that usually occur in two sets form a closely spaced network called cleats. The two sets of fractures are, in most instances, mutually perpendicular and also perpendicular to bedding. The through-going and well-developed cleats formed first and are termed face cleats. The cleats that often terminate at the face cleats formed later and are called butt cleats. The cleat system provides an essential and effective flow path for gas, and much of the measured bulk or "seam" permeability is due to the cleat system, although the presence of larger scale discontinuities such as fractures, joints, and faults can also make a significant contribution. The coal matrix is separated by the natural fracture network and is the principal medium for storage of the gas, principally in adsorbed form and with low permeability in comparison with the bounding cleats (Gray 1987). The surface area of the coal on which the methane is adsorbed as a liquid-like, monomolecular layer is very large (20–200 m^2/g) (Patching 1970). The remaining gas exists in the natural fracture systems, or cleats, either as free gas or in solution in any water present.

The concept of injecting carbon dioxide into coal seams is considered to be a safe and effective method for permanent

W. C. Zhu (✉) · C. H. Wei · T. Xu
Key Laboratory of Ministry of Education on Safe Mining
of Deep Metal Mines, Northeastern University,
Shenyang 110819, China
e-mail: zhuwancheng@mail.neu.edu.cn

J. Liu
School of Mechanical and Chemical Engineering,
The University of Western Australia, Crawley,
WA 6009, Australia

D. Elsworth
Energy and Mineral Engineering and G3 Center,
Penn State University, University Park, PA 16802, USA

storage of the CO_2 in coal seam with the added benefit of enhancing coalbed methane (ECBM) production (Durucan et al. 2009). During the injection of CO_2, one key issue that must be addressed is coal permeability, because high coal permeability is required for sufficient and practical injectivity of CO_2 into coal seams and for efficient recovery of CH_4 (Cui et al. 2007; Liu and Rutqvist 2010). In this respect, coal swelling/shrinking due to gas adsorption/desorption is a well-known phenomenon and is regarded as a key component for coal reservoir permeability behavior during primary and enhanced coalbed methane (CBM) recovery (Pan and Connell 2007). Results from laboratory experiments reported by Robertson and Chrisiansen (2005), as well as other field and laboratory observations, such as those conducted by Pan and Connell (2011), Wang et al. (2010), Cui and Bustin (2005) and Mavor and Vaughn (1997), indicate that as gas pressure is increased under conditions of constant applied stress, coal permeability initially reduces until a peak is approached, and then rebounds with the increasing gas pressure (Robertson and Chrisiansen 2005).

This kind of permeability evolution is controlled by at least two mechanisms (Liu and Rutqvist 2010; Izadi et al. 2011; Pan and Connell 2012): (1) gas pressure increase, which tends to mechanically open coal cleats (fractures) and thus enhance coal permeability; and (2) adsorption of gas into coals, which induces swelling in the coal matrix (volumetric strain) and thus reduces coal permeability by narrowing and even closing fracture (cleat) apertures. Palmer and Mansoori (1998) described a permeability model incorporating the combined effect of the elastic properties of coal and gas adsorption on the resulting matrix strain, which includes a permeability loss term due to an increase in effective stress, and a permeability gain term resulting from matrix shrinkage as gas desorbs from the coal. Cui and Bustin (2005) investigated quantitatively the effects of gas reservoir pressure and adsorption-induced volumetric strain on coal-seam permeability with constraints from the measurement of adsorption isotherm and associated volumetric strain, based on which a stress-dependent permeability model is derived (Cui and Bustin 2005).

Liu and Rutqvist (2010) developed a coal-permeability model for uniaxial strain and constant confining-stress conditions, which explicitly considers fracture–matrix interaction during coal-deformation processes and is based on a newly proposed internal swelling stress concept to account for the impact of matrix swelling (or shrinkage) on fracture–aperture changes resulting from partial separation of matrix blocks by fractures that do not completely cut through the whole matrix. Connell et al. (2010) presented two new analytical permeability models, derived from the general linear poroelastic constitutive law, which include the effects of triaxial strain and stress for coal undergoing gas adsorption-induced swelling.

In our previous studies (Liu et al. 2011; Izadi et al. 2011), the interactions of the fractured coal mass in which cleats do not create a full separation between adjacent matrix blocks due to the presentence of solid rock bridges was considered. When the coal matrix swelling is localized in the vicinity of a fracture, the effect of swelling acts competitively over two components: increasing porosity/permeability due to the swelling of the bridging contacts and reducing porosity/permeability due to the swelling of the intervening free-faces. When the coal matrix swelling is de-localized from the vicinity of a fracture compartment to the external boundary, the coal bridge swelling increases the fracture aperture while the coal matrix swelling changes the spacing only. It implies that the transient characteristics of coal permeability are likely controlled by the localized swelling near the vicinity of coal fracture voids rather than the outside boundaries (Liu et al. 2011; Izadi et al. 2011). In addition, current laboratory measurements are only designed for determining the permeability at the final equilibrium states. For homogeneous coal samples, a net increase in permeability should be observed theoretically in these tests. However, this condition may never be achieved for real coal samples. In this respect, a difference of the ultimate permeability between an ideal homogeneous coal and a real heterogeneous coal is expected.

As observed in previous studies (Karacan 2003, 2007; Karacan and Mitchell 2003), the CO_2 adsorption-associated volumetric strains in coal under constant effective stress are heterogeneous processes depending on the lithotypes. These observations may have implied that the swelling component of matrix swells while the non-swelling component of matrix is compacted in response. This provides the basis to assume that coal swelling is a heterogeneous process depending on the distribution of coal voids such as fractures and that coal matrixes show the highest degree of swelling due to adsorption of CO_2 while fractures are compressed in response. Wu et al. (2011) represents heterogeneous swelling processes through the inclusion of spatially distributed fracture porosity into complex interactive phenomena (mechanical coupling with gas transport). Their model results illustrate the crucial role of heterogeneous swelling in generating swelling-induced reductions in permeability even when the fractured sample is mechanically unconstrained. These results prove that coal swelling is a heterogeneous process depending on the distribution of coal voids: matrix (swelling component) swells while fractures (non-swelling component) are compacted in response.

Recently, Izadi et al. (2011) proposed a model in which the coal heterogeneity was represented by the specified damage zone in the vicinity of fracture walls. This representation is consistent with the reported experimental observation (Ranjith et al. 2010; Vinokurova and Ketslakh

1985; Viete and Ranjith 2006; Perera et al. 2011). In the damage zone both the Langmuir swelling coefficient and the Young's modulus change according to the pre-defined functions. However, as a matter of fact, the damage zone cannot be pre-defined because it is dependent on the stress or strain state within the coal matrix. In this study, we develop a coupled coal–gas interaction model that incorporates the material heterogeneity and damage evolution of coal, which allows us to couple the progressive development of damage zone with gas adsorption progresses within the coal matrix. The coupled model was used to evaluate the impact of coal damage on the evolution of coal permeability. This goal is achieved through explicit simulations of the dynamic interactions between coal matrix swelling and fracture aperture alteration due to the coal matrix damage, and translations of these interactions to permeability evolution under unconstrained swelling.

2 Governing Equations

2.1 Characterization of Coal Sample Heterogeneity

The coal sample is assumed to be heterogeneous and isotropic with its mechanical properties assigned randomly from a Weibull statistical distribution as defined in the following probability density function (Zhu and Tang 2004):

$$f(u) = \frac{m}{u_0} \left(\frac{u}{u_0}\right)^{m-1} \exp\left(-\left(\frac{u}{u_0}\right)^m\right) \quad (1)$$

where u is the mechanical parameter of an individual element (such as elastic modulus or uniaxial compressive strength) in the numerical sample, u_0 is the scale parameter related to the average of the element parameters, and the shape parameter m reflects the degree of material homogeneity and is defined as a homogeneity index. More detailed description about this can be referred in Zhu and Tang (2004).

2.2 Mechanical Equilibrium Equation

From the equilibrium condition of an infinitesimal element in the porous medium assumed elastic, the deformation model of the porous medium can be derived and expressed in terms of displacement under a combination of changes of applied stresses (positive for tension) and gas pressures (negative for suction) as follows (Zhu et al. 2011):

$$G u_{i,jj} + \frac{G}{1-2v} u_{j,ji} - \alpha_{p,i} - K\varepsilon_{s,i} + f_i = 0 \quad (2)$$

where u_i ($i = x, y, z$) is displacement of the medium in the $x, y,$ and z directions, G is shear modulus of coal, p is gas

pressure, v is the Poisson's ratio of coal, K is the bulk modulus of coal, ε_s is volumetric matrix strain induced by gas adsorption, f_i is the components of the net body force in the $x, y,$ and z directions, and parameter α (≤ 1) is Biot's coefficient, which depends on the compressibility of the constituents and can be defined as (Biot 1941)

$$\alpha = 1 - \frac{K}{K_s}, \quad (3)$$

where K_s is the effective bulk modulus of the coal matrix.

The macroscopic volumetric matrix swelling strain ε_s induced by gas desorption from coal, is assumed to be (Levine 1996)

$$\varepsilon_s = \varepsilon_L \frac{p}{p + p_L}. \quad (4)$$

where ε_L and p_L represents the Langmuir strain constant and Langmuir pressure constant (Pa), respectively.

2.3 Damage Evolution and its Effect on Elastic Modulus

As illustrated in Fig. 1, the damage of coal in tension or shear is initiated when its state of stresses satisfies the maximum tensile stress criterion or the Mohr–Coulomb criterion, respectively, as expressed by (Zhu and Tang 2004):

$$\begin{aligned} & F_1 \equiv \sigma_1 - f_{t_0} = 0 \quad \text{or} \\ & F_2 \equiv -\sigma_3 + \sigma_1((1+\sin\phi)/(1-\sin\phi)) - f_{c_0} = 0, \end{aligned} \quad (5)$$

where σ_1, σ_3 are major principal stress and minor principal stress, respectively, ϕ is internal cohesive angle, f_{t_0} and f_{c_0} are the uniaxial tensile and compressive strength, respectively, and F_1 and F_2 are two damage threshold functions.

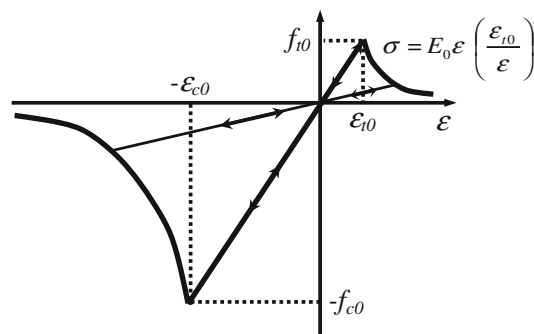The elastic modulus of an element degrades monotonically as damage evolves and is derived as follows:

Fig. 1 The elastic damage-based constitutive law of elements under uniaxial stress condition (f_{t_0} and f_{c_0} are uniaxial tensile strength and uniaxial compressive strength, respectively)

$$E = (1 - D)E_0 \tag{6}$$

where D represents the damage variable, and E and E_0 are the elastic modulus of the damaged and the undamaged coal, respectively. Under any stress conditions, the tensile stress criterion is applied preferentially. In this regard, as shown in Fig. 1, the damage variable can be calculated as follows (Zhu and Tang 2004):

$$D = \begin{cases} 0 & F_1 < 0 \text{ and } F_2 < 0 \\ 1 - \left| \dfrac{\varepsilon_{t0}}{\varepsilon_1} \right|^n & F_1 = 0 \text{ and } \mathrm{d}F_1 > 0 \\ 1 - \left| \dfrac{\varepsilon_{c0}}{\varepsilon_3} \right|^n & F_2 = 0 \text{ and } \mathrm{d}F_2 > 0 \end{cases} \tag{7}$$

where ε_1 and ε_3 are major principal strain and minor principal stain, respectively. ε_{t0}, and ε_{c0} are the maximum principal strain in tension and the maximum principal strain in compression when damage occurs according to the maximum tensile stress criterion and Mohr–Coulomb criterion, respectively, and n is a constitutive coefficient with a value of 2.0 (Zhu and Tang 2004).

2.4 Effect of Matrix Swelling on Fracture Permeability

The coal is composed of a solid matrix which contains interstitial pore space filled with a freely diffusing pore gas. The permeability of coal sample may be defined through the cubic law for fracture permeability as (Witherspoon et al. 1980)

$$k = \frac{b^3}{12s}, \tag{8}$$

enabling aperture to be defined as

$$b_0 = \sqrt[3]{12k_0 s} \tag{9}$$

where b is aperture (m), k is permeability of coal sample (m²), and s is side length of the coal sample (as shown in Fig. 2a). Correspondingly, b_0 and k_0 are initial aperture of fracture and corresponding permeability.

The dynamic permeability of the cracked system may be expressed as

$$\frac{k}{k_0} = \left(1 + \frac{\Delta b}{b_0} \right)^3. \tag{10}$$

The aforementioned Eq. (2), together with damage evolution (Eqs. 6 and 7), are nonlinear partial differential equations (PDEs) with second order for space, and difficult to solve theoretically. In this respect, the complete set of coupled equations is implemented into, and solved by using COMSOL Multiphysics, a powerful PDE-based multiphysics modeling environment (COMSOL 2008).

3 Numerical Simulations

The dual-porosity fractured model we used in this paper is from Izadi et al. (2011), as shown in Fig. 2. The model contains an elliptical fracture with the semi-major axis of 0.25 mm and semi-minor axis of 0.05 mm within a 1 mm × 1 mm domain. The fracture width is assumed as $a = 0.5$ mm. The fracture aperture is assumed as $b = 0.1$ mm. Other related parameters used in the numerical simulations are listed in Table 1 (Durucan et al. 2009; Robertson and Chrisiansen 2005).

As shown in Fig. 2b, the external boundary of the model is free to deform but under invariant total boundary stresses, i.e. $\sigma_{bx} = 10$ MPa and $\sigma_{by} = 10$ MPa. A gas pressure of p is applied at both the internal and external boundaries; thus the whole domain seems to be immersed in the gas reservoir with a constant gas pressure of p. In this respect, the gas flow is not affected by the deformation and damage of coal matrix; however, the gas adsorption or desorption may alter the deformation and damage of coal matrix.
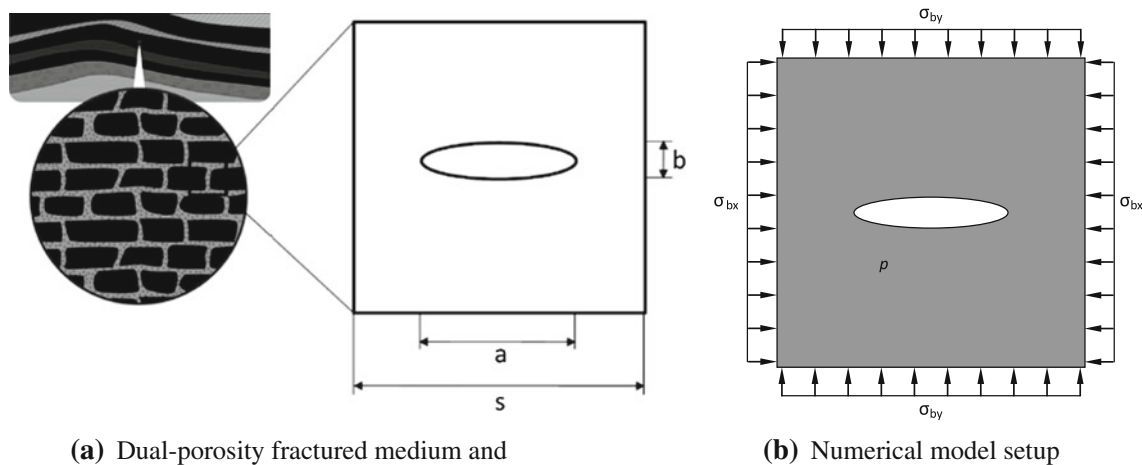

(a) Dual-porosity fractured medium and

(b) Numerical model setup

Fig. 2 Diagram for a dual-porosity fractured medium and b numerical model setup (Izadi et al. 2011)

Table 1 Parameters used in the numerical simulation

Symbol	Description	Value	Units
E	Young's modulus of coal	2	GPa
υ	Poisson's ratio of coal	0.34	–
p_L	Langmuir pressure constant	2.0	MPa
ε_L	Langmuir volumetric strain constant	0.02	–
α	Biot's coefficient	0.6	–

The inner fracture is full of free gas with pressure of p, which tends to mechanically dilate coal fracture. The free gas can diffuse and adsorb into the coal matrix or fracture, which can reduce swelling in the coal matrix. These two mechanisms may interact with each other to vary the facture aperture and coal permeability.

In this section, we first briefly review the models proposed recently by Izadi et al. (2011) (namely Scenarios I and II). Second, a damage-based model as formulated in Sect. 2.3 is used to study the damage evolution process and resultant fracture aperture change under the combined contribution of external load and gas pressure (Scenario III). Third, the effect of different values of Langmuir strain constant ε_L on damage zone and aperture is examined (Scenarios III and IV). Fourth, allowing for different in situ stress condition, the effect of different lateral pressure coefficients on damage zone and aperture is analyzed further (Scenarios III and V). At last, to examine the effect of coal seam heterogeneity on the damage and permeability variation, another model with different values of homogeneity index m is solved (Scenario VI).

3.1 Scenario I: Homogeneous Elastic Model ($\varepsilon_L = 0.02$)

First we consider the sample with homogeneous elastic modulus and swelling coefficient. Figure 3a shows the resulting displacement and deformation of the model when the gas pressure in the fracture is up to 8.0 MPa. It is obviously observed from Fig. 3a that the whole sample swells outwards with increasing gas pressure.

Figure 3b shows the relation between change of aperture and matrix pore pressure, where Δb denotes the change of aperture with positive value for "opening" and negative value for "closing". When the initial stress is applied on the model, the sample is compacted and the fracture aperture decrease about 5.5 μm. In this respect, the aperture and permeability under this initial stress and zero gas pressure are considered as their initial conditions. Then, during the increase of applied gas pressure, the sample dilates outwards and the aperture increases linearly, thus leading to the increase of the aperture and permeability. In this respect, this numerical result is identical to that presented by Izadi et al. (2011).

3.2 Scenario II: Elastic Model with a Prescribed Damage Zone ($\varepsilon_L = 0.02$)

We extend the model in Scenario I to reproduce the behavior of numerical sample with a prescribed damage zone around the fracture. As proposed by Izadi et al. (2011), the Langmuir swelling coefficient decreases outwards from the wall and the Young's modulus increases outwards from the wall, i.e.
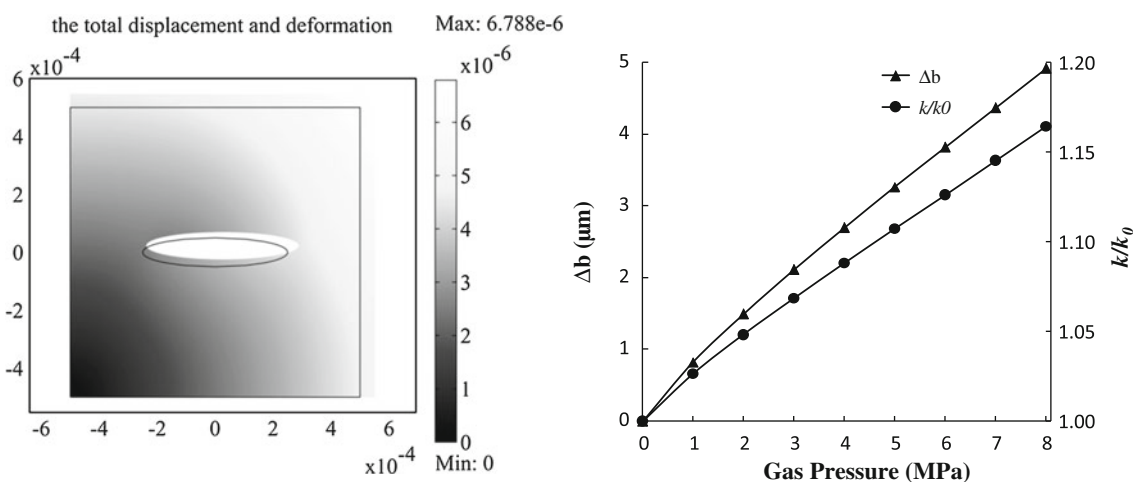

(a) Total displacement and deformation   **(b)** Variation of aperture and permeability

Fig. 3 Numerical results for Scenario I: **a** total displacement and deformation, **b** variation of aperture and permeability with gas pressure

$$E = E_0 \cdot \frac{r}{s/2} = E_0 \cdot \frac{2r}{s}, \quad \varepsilon_L = \varepsilon_{L_0} \cdot \frac{s}{2r} \qquad (11)$$

where $r = \sqrt{x^2 + y^2}$ is the distance from the center of the model, s is the width of matrix block, and E_0 and ε_{L_0} are initial Young's modulus and Langmuir swelling coefficient of coal matrix, and E and ε_L are damaged Young's modulus and Langmuir swelling coefficient of coal matrix. In this regard, the damage variable can be expressed as $D = 1 - E/E_0$. The prescribed distribution of Young's modulus and Langmuir swelling coefficient are shown in Fig. 4a, b. The distribution of Young's modulus is similar to the damage zone.

When these kind of prescribed damage zone and associated distribution of Young's modulus and Langmuir swelling coefficient are assigned, the change of aperture and permeability with increasing gas pressure is shown in Fig. 4c. It is predicted that, as gas pressure is increased, the

aperture initially reduces as the material in the wall swells and this swelling is constrained by the far-field modulus. As the peak Langmuir strain is approached, the decrease in the fracture aperture halts and aperture increases with pressure. In this respect, from the numerical model used in this work, the same conclusion as that presented by Izadi et al. (2011) is drawn. This can further validate that the proposed model is correct and effective in predicting the variation of aperture and permeability with the gas pressure.

3.3 Scenario III: Heterogeneous Model with Damage Analysis ($\lambda = 1.0$, $\varepsilon_L = 0.02$)

During the calculation in Scenario II, the damage zone is prescribed, and a lateral pressure coefficient of 1.0 is assigned, to simplify the theoretical analysis. However, as mentioned in Sect. 2.3, the damage zone distribution is rigorously controlled by the stress or strain distribution
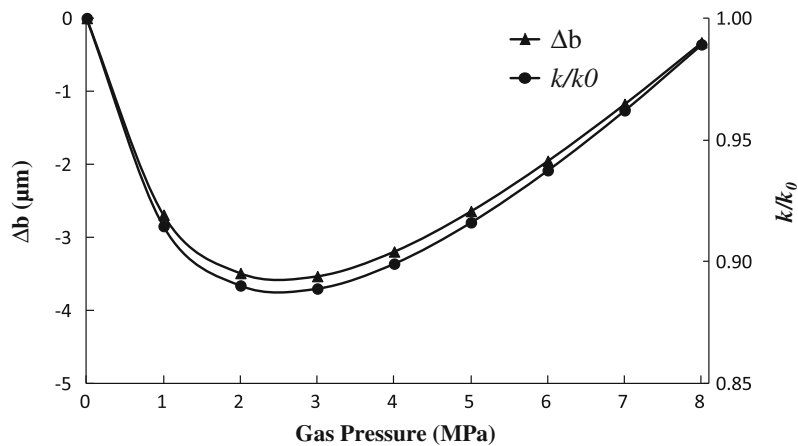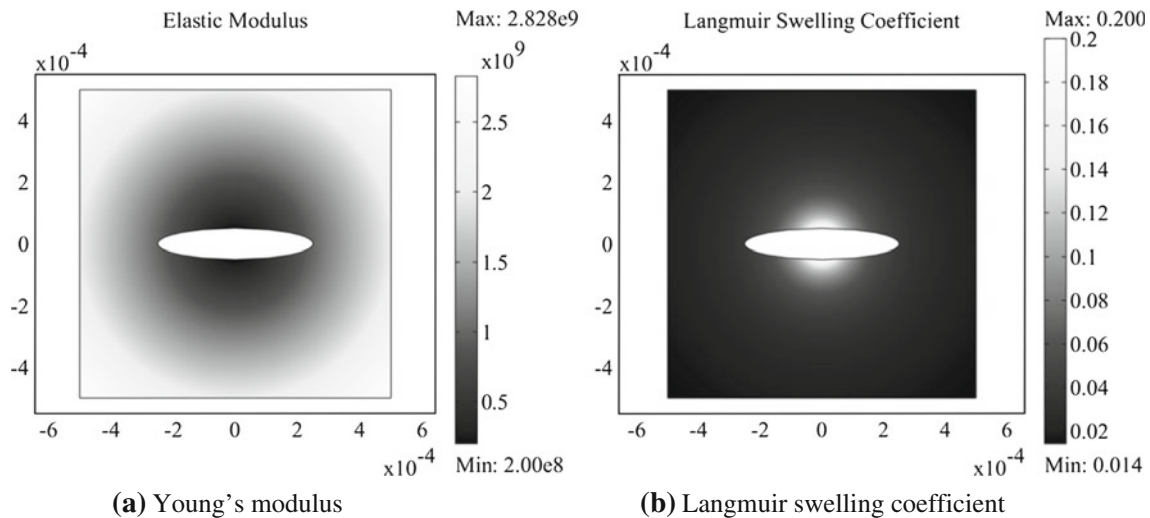

(a) Young's modulus

(b) Langmuir swelling coefficient

(c) Variation of aperture and permeability

Fig. 4 Prescribed distribution of **a** Young's modulus and **b** Langmuir swelling coefficient for Scenario II according to Izadi et al. (2011), **c** the predicted variation of aperture and permeability with gas pressure

around the fracture. Most importantly, the boundary conditions, such as lateral pressure coefficient, may significantly alter the stress and damage zone distribution around the fracture. Therefore, relaxation of the above two assumptions, i.e. the damage zone distribution and Langmuir swelling coefficient as expressed by Eq. (11), is important to examine this issue more rigorously.

In this section, the numerical model as proposed in Sect. 2.3 is used to calculate the damage zone distribution, based on which the aperture change is predicted. Up to now, there is no rigorous evidence to confirm the dependence of Langmuir swelling coefficient of coal matrix on the damage of coal seam; therefore, only the damage-dependent elastic modulus is taken into account in the numerical analysis. The coal sample is assumed to be heterogeneous with its elastic modulus specified according to a Weibull distribution and the homogeneity index m equals 6.0 (Fig. 5a). In this scenario, the boundary stress of 1.0 MPa per step is applied in Y direction until Step 10 (i.e. the final boundary stress of 10.0 MPa is attained), and then it is followed by the increasing gas pressure of 1.0 MPa per step until the prescribed gas pressure is attained. For example, at Step 11, both the boundary stress of 10.0 MPa and gas pressure of 1.0 MPa are applied simultaneously.

Figure 5b shows the variation of aperture and permeability with respect to gas pressure, which indicates that as gas pressure is increased, coal permeability initially reduces until a peak is approached, and then rebounds with the increasing gas pressure. That is to say, the permeability evolution, similar to Fig. 4c is captured by the damage model when the heterogeneity of coal seam is considered, even though the assumption of damage-dependent Langmuir swelling coefficient, as proposed by Izadi et al. (2011), is not incorporated. Figure 5c shows the damage zone distribution, in which the tensile and shear damages are denoted with negative and positive numbers ranging from −1.0 to 1.0. As shown in Fig. 5c, at Step 10 (only external boundary loading is exerted), no damage zone is provoked. However, after the gas pressure of 1.0 MPa is applied at Step 11, the damage initiates around the existing facture under the combined contribution of expansion induced by the free gas and swelling of the coal matrix induced by gas adsorption, leading to the decline of elastic modulus in the damage zone. In this respect, gas adsorption induced swelling in the damage zone is constrained by the far-field modulus, the adsorption-induced strain in coal matrix is more salient than the contribution of gas pressure to extend the fracture, a larger area of damage zone is induced around the fracture, resulting in the fracture face swelling inwards.

The aperture of the sample declines, so does the permeability, until a minimum k/k_0 of 94 %. When the gas pressure exceeds 4.0 MPa, the contribution of free gas dominates, leading to the increase of aperture and permeability until the final value of k/k_0 of 107 %. During this process, as external load is applied on the sample and gas pressure is increased, damage zone firstly initiates at the location with low curvature around the fracture, which is rigorously governed by the stress or strain states. The damage zone may propagate further with the increasing gas pressure. In this scenario, the damage zone distribution is rigorously related to the stress/strain distribution and heterogeneity in the sample, therefore the aperture and permeability respond differently from that in Fig. 4c, is numerically predicted.

3.4 Scenario IV: Heterogeneous Model with Damage Analysis under Different ε_L ($\lambda = 1.0$)

Robertson (2005) found that, regardless of the amount of decrease in strain resulting from an increase in coal rank, the strain of all three gases (i.e. CH_4, CO_2 and N_2) did decline as rank increased. In this respect, CH_4-induced strain decreases only slightly with the increasing coal rank, but the CO_2- and N_2-induced strain curves each decrease by a factor of about two. However, Bustin (2002) compared the adsorption capacity (not strain) of coals with different ranks and found a trend towards higher capacity with higher coal rank. Thus, the Langmuir strain may be related to the coal rank; however, there is no well-accepted relation between them. In this Scenario IV, ε_L is assigned to be 0.01 and 0.04, respectively, to examine the effects of Langmuir strain constant ε_L on the damage zone distribution and fracture aperture change.

As shown in Fig. 6a, when Langmuir strain constant ε_L is 0.01, the damage zone around the fracture is developed in a very small area; the dilation of coal seam induced by gas adsorption is very weak. Thus, the expansion induced by the free gas in the fracture is the dominant mechanism to govern the aperture opening. As a result, it is found that the aperture and permeability increase continuously with the gas pressure (Fig. 6b). This behavior is similar to that in Fig. 3, where no damage zone is considered around the fracture.

As for ε_L of 0.04, the damage does not initiate under the external boundary stress; however, as shown in Fig. 6c, when the gas pressure is applied at Step 11, a large damage zone is induced around the fracture, resulting in the fracture face swelling inwards. In this respect, the adsorption-induced strain in coal matrix is more salient than the contribution of free gas pressure to extend the fracture, and the fracture may close due to the swelling of the coal matrix resulting in the sharp decline of aperture and permeability until the fracture closes.

Therefore, the evolution of aperture and permeability of fractured coal sample is mainly controlled by the damage zone developed around the fracture. Figures 3b and 6d
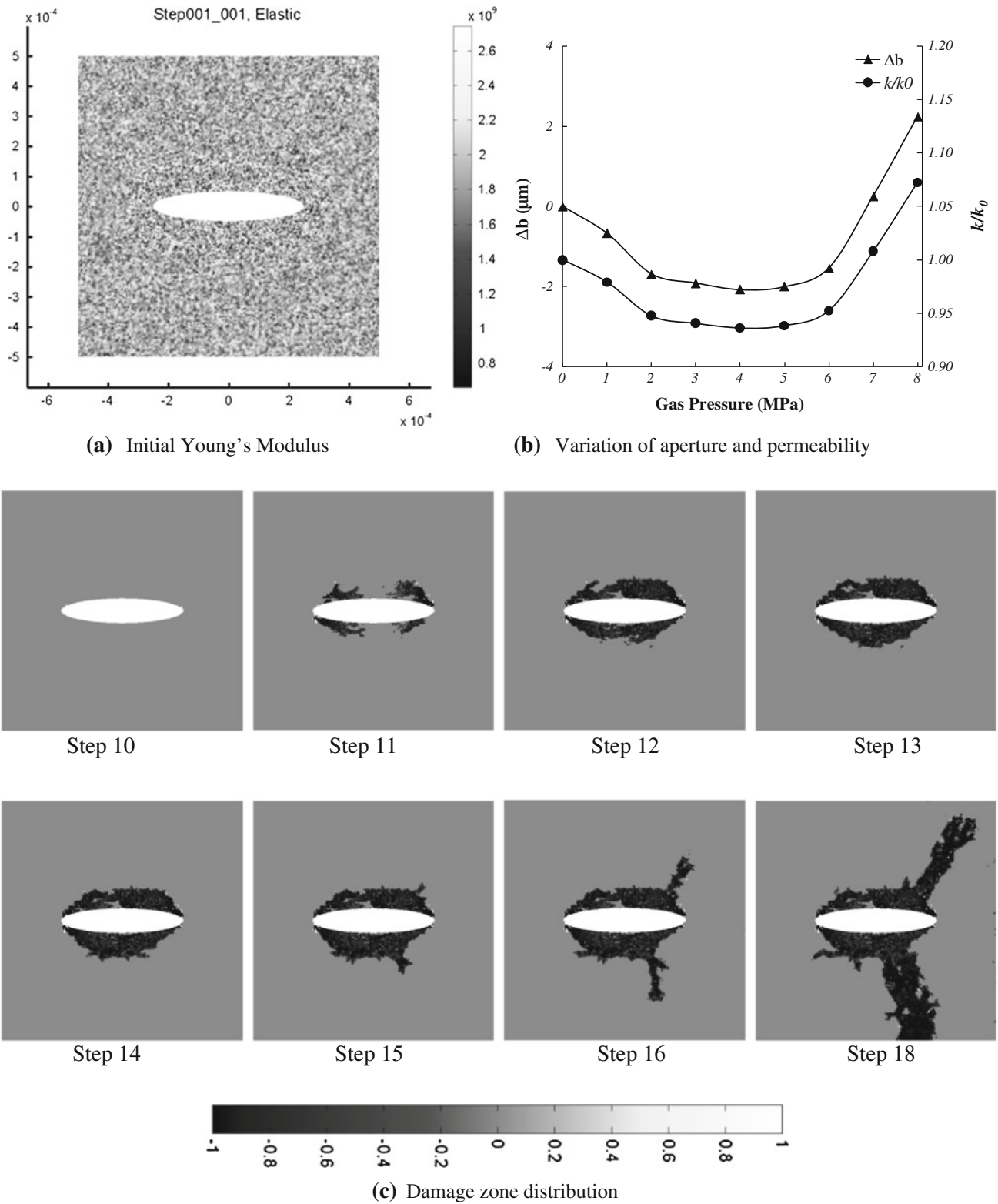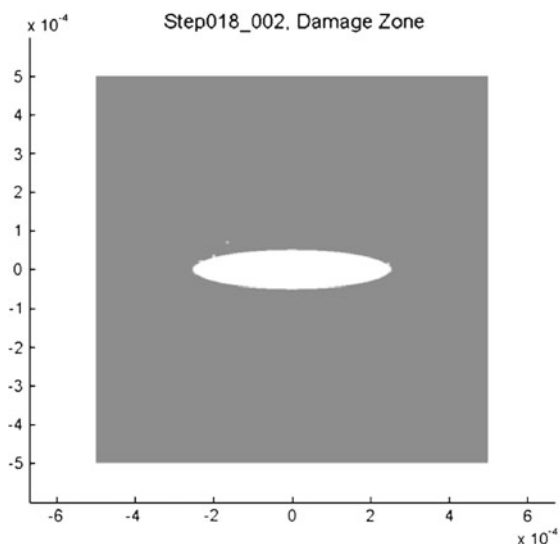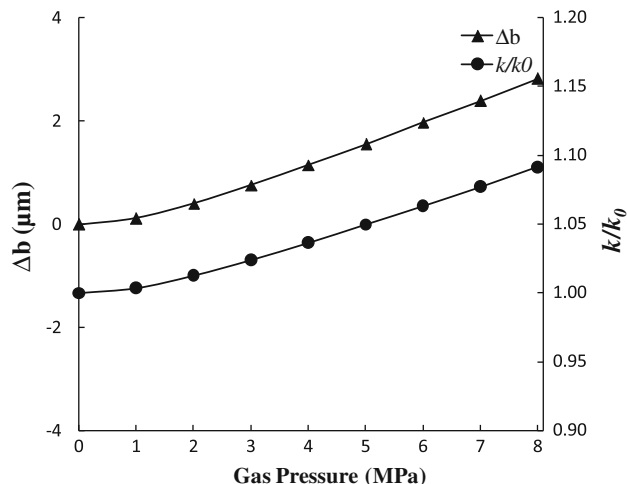
(a) Initial Young's Modulus (b) Variation of aperture and permeability

Step 10   Step 11   Step 12   Step 13

Step 14   Step 15   Step 16   Step 18

(c) Damage zone distribution

Fig. 5 Numerical results for Scenario III: **a** initial Young's modulus, **b** variation of aperture and permeability with gas pressure, and **c** damage zone distribution
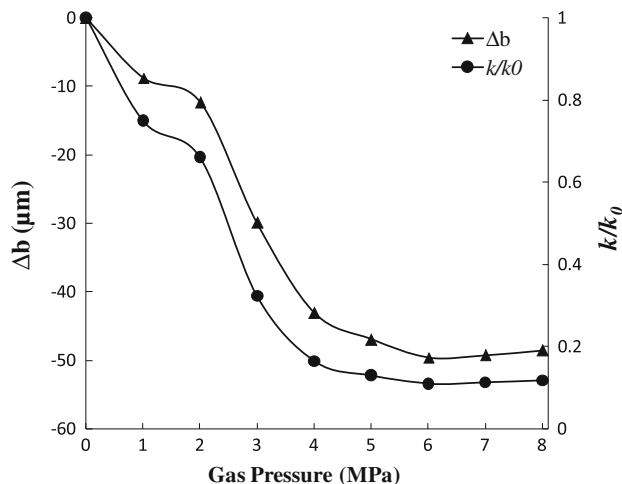
(a) Damage zone at Step 18 for $\varepsilon_L = 0.01$

(b) Variation of aperture and permeability for $\varepsilon_L = 0.01$
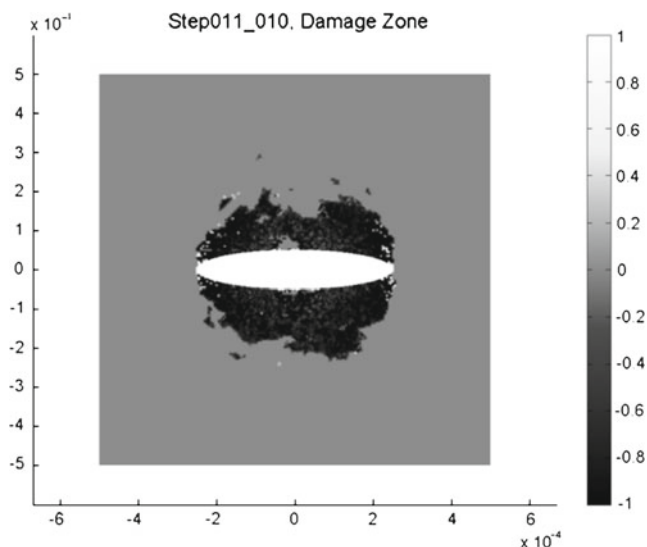
(c) Damage zone at Step 11 for $\varepsilon_L = 0.04$

(d) Variation of aperture and permeability for $\varepsilon_L = 0.04$

Fig. 6 Numerical results for Scenario IV: **a** damage zone distribution and **b** variation of aperture and permeability for $\varepsilon_L = 0.01$; **c** damage zone distribution and **d** variation of aperture and permeability for $\varepsilon_L = 0.04$

represent two extreme conditions where the damages are not developed and fully developed, respectively. In this regard, as shown in Figs. 5 and 6, the damage-based model enables us to capture the possible aperture and permeability evolution due to the damage zone development depending on the stress and strain conditions around the existing fracture in coal sample.

3.5 Scenario V: Heterogeneous Model with Damage Analysis for $\lambda = 2.0$ ($\varepsilon_L = 0.02$)

In the previous analysis, the coal sample is assumed to be under a hydrostatic stress state, i.e. lateral pressure

coefficient λ is 1.0. However, the in situ stress condition, denoted with lateral pressure coefficient λ, may alter the stress condition around the fracture a lot. Therefore, allowing for non-hydrostatic stress state may lead to quite different damage zone distribution around the fracture. In this respect, as an example, a lateral pressure coefficient λ of 2.0 is specified. The boundary stresses, i.e. $\sigma_{bx} = 20.0$ MPa and $\sigma_{by} = 10.0$ MPa, is applied at the boundary of domain.

As shown in Fig. 7a, the damage zone hardly initiates around the fracture after the external load is applied at Step 10, which does not change the aperture at all. The application of the gas pressure at Step 11 provokes the salient extension of damage zone (Fig. 7a); therefore, the aperture

decreases obviously. However, after the gas pressure of 3.0 MPa, the damage zone does not extend further. As shown in Fig. 7b, during the increase of gas pressure, the aperture initially reduces until a minimum value of $k/k_0 = 69\%$ as the material in the damage zone swells and this swelling is constrained by the far-field boundary. When the peak Langmuir strain is approached, the decrease in the fracture permeability halts and permeability increases a bit until $k/k_0 = 71\%$, indicating that the effect of adsorption-induced strain is very limited, partly because the damage zone halts to extend under the gas pressure higher than 3.0 MPa. In this Scenario V, because the damage zone does not extend further when gas pressure is larger than 3.0 MPa, the final aperture/permeability is quite smaller than the initial ones, denoting the weak expansion induced by the free gas, compared with the swelling of the coal matrix induced by gas adsorption.

3.6 Scenario VI: Heterogeneous Model with Damage Analysis for $m = 3.0$ ($\lambda = 1.0$, $\varepsilon_L = 0.02$)

As mentioned in Sect. 2.1, a smaller homogeneity index m for Weibull distribution implies a more heterogeneous numerical sample and vice versa. In Scenarios III–V, the values of m equal 6.0, denoting a relatively homogeneous coal matrix (Zhu and Tang 2004). In this scenario m is assigned to 3.0, in order to study the effect of heterogeneity on damage zone distribution and fracture aperture. The initial Young's modulus distribution is shown in Fig. 8a.

Comparing with Fig. 5 in the Scenario III with $m = 6.0$, the coal sample in this scenario is more heterogeneous (Fig. 8a), which results in a large area of random damages around the fracture (as shown in Fig. 8c). It denotes that for more heterogeneous coal stronger gas adsorption influence on permeability may occur. Therefore, both the minimum and final values of k/k_0, reaching 85 and 87 % (Fig. 8b), respectively, are lower than those in the Scenario III ($m = 6.0$).

In this study, the coal heterogeneity could affect the stress distribution and damage evolution, thus altering the aperture and permeability of coal sample. Based on this, one possible mechanism clarified from this numerical simulation is that the more heterogeneous coal sample has more fractures or discontinuities to provide more space for gas movement and consequently it has higher gas adsorption and greater permeability variation.

4 Comparison with Experimental Observation

For the mechanical model as proposed by Izadi et al. (2011) as shown in Fig. 2, the permeability of this sample is dependent on the damage zone development around the existing fracture; it may increase monotonously (Figs. 3b, 6b), decrease until a peak then increases (Figs. 4c, 5b, 7b, 8b), and decrease monotonously (Fig. 6d). Different tendencies predicted with different input parameters could be used to clarify possible mechanism responsible for the permeability evolution phenomenon observed in the experiments.

In this section, the injection of CH_4 into Anderson 01 Core experimented by Robertson and Chrisiansen (2005) is predicted with the numerical simulation. For the boundary conditions, a constant overburden pressure of 6.9 MPa (with a lateral pressure coefficient λ of 1.0) and varying pore gas pressure between 0.69 and 5.5 MPa are specified. As shown in Fig. 9, the numerical simulation predicts the tendency of permeability variation although the permeability increase at the higher gas pressure is underestimated. This denotes that the reasonable validation of parameters used in the coupled coal–gas interactions model during the deformation and damage of coal seam is necessary to fully capture this mechanism quantitatively.

5 Conclusions

A fully coupled coal–gas model is developed to resolve why coal permeability changes instantaneously from reduction to enhancement under the constant effective stress condition as widely reported in the literature. This goal is achieved through explicit simulations of the dynamic interactions between coal matrix swelling induced damage and fracture aperture alteration, and translations of these interactions to permeability evolution under the constant effective stress condition. Based on the evaluation results, the evolution of coal permeability under the influence of gas adsorption is controlled primarily by the following factors:

- Evolution of coal damage zone: coal is a typical dual porosity/permeability system containing porous matrix surrounded by fractures. Our results demonstrate that the evolution of damage zone around the coal fracture wall controls the complex evolution of coal permeability under the influence of gas adsorption. This influence is regulated by the external boundary conditions.
- External boundary conditions: The transition of coal matrix damage zone from local damage within the vicinity of a fracture to global damage controls the simultaneous switching of coal permeability from the initial reduction to the late recovery. At the initial stage of gas adsorption, matrix damage is localized within the vicinity of the fracture compartment. As the gas pressure increases, the localized damage zone widens further into the matrix and becomes global
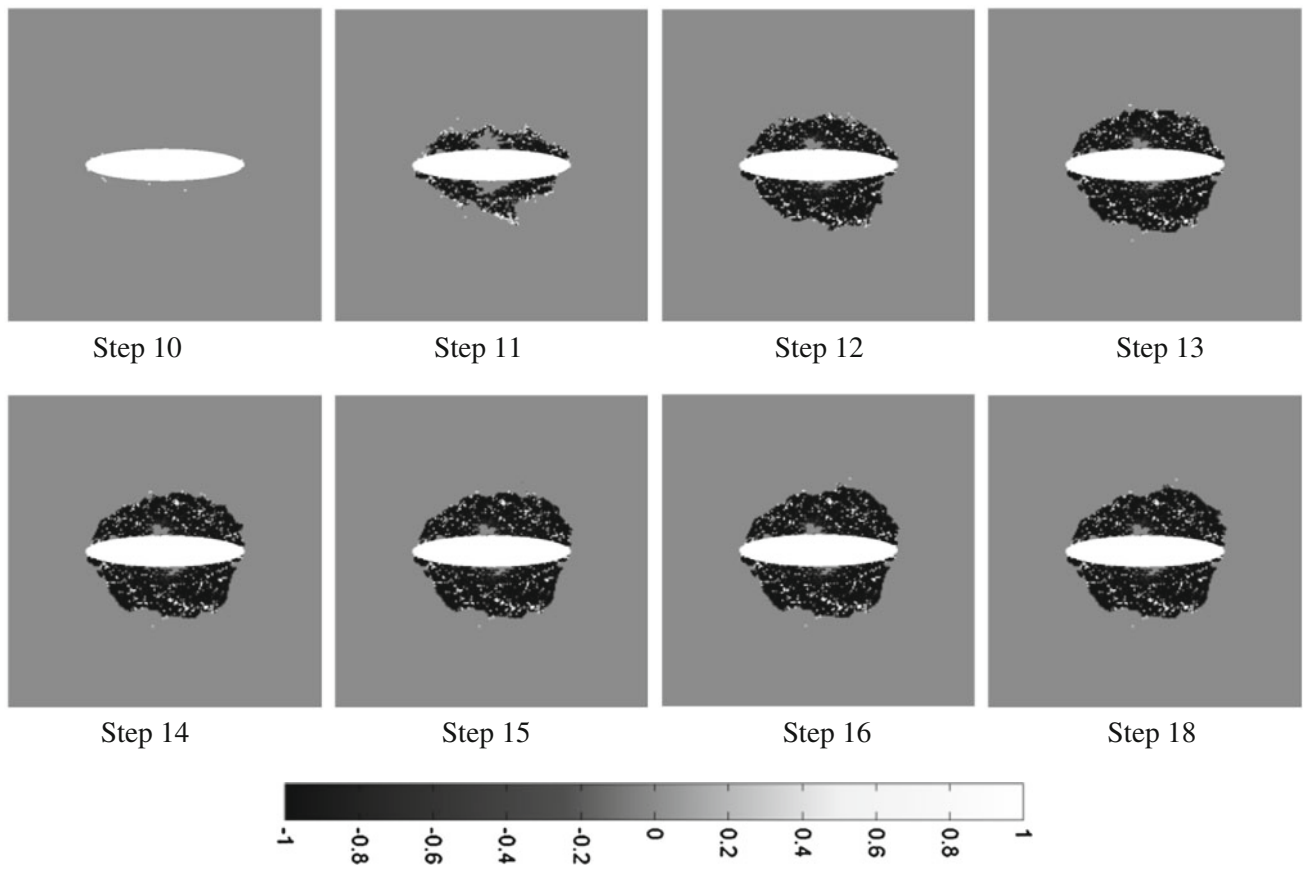
(a) Damage zone distribution
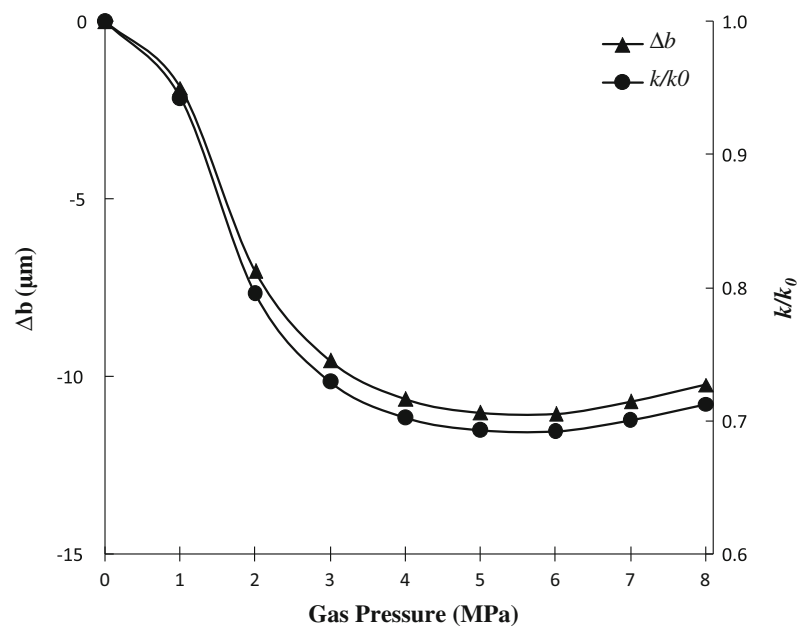
(b) Variation of aperture and permeability

Fig. 7 Numerical results for Scenario V: **a** damage zone distribution and **b** variation of aperture and permeability with gas pressure under the lateral pressure coefficient λ of 2.0
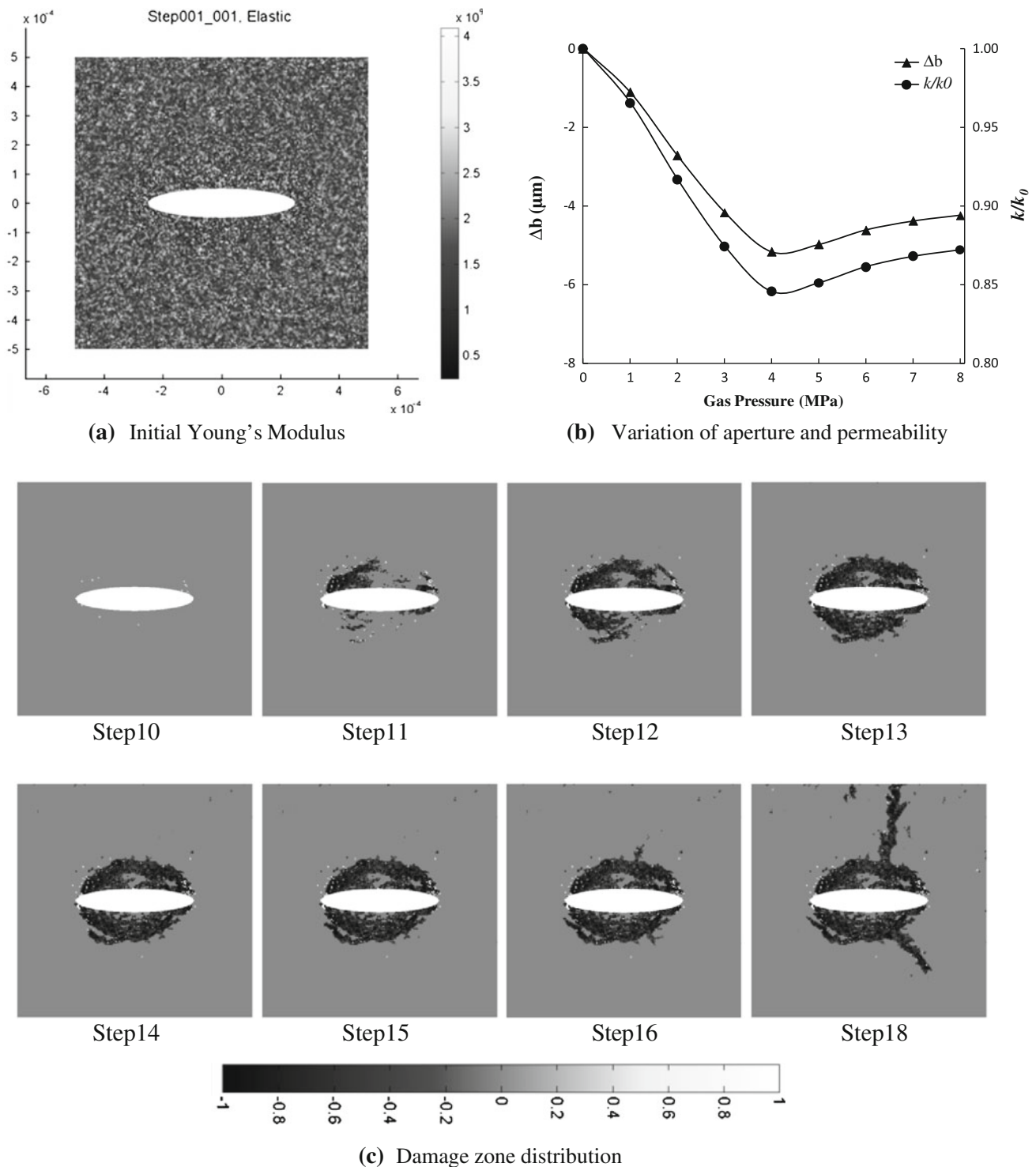
(a) Initial Young's Modulus

(b) Variation of aperture and permeability

(c) Damage zone distribution

Fig. 8 Numerical results for Scenario VI: **a** initial Young's modulus, **b** variation of aperture and permeability with gas pressure and **c** damage zone distribution for a homogeneity index $m = 3.0$

damage. During the formation of localized damage zone, coal permeability is controlled by the internal fracture boundary condition and behaves volumetrically; while during the formation of global damage zone, coal permeability is controlled by the external boundary condition.

• Coal matrix swelling/shrinking: the evolution of coal matrix swelling/shrinking is the primary process that
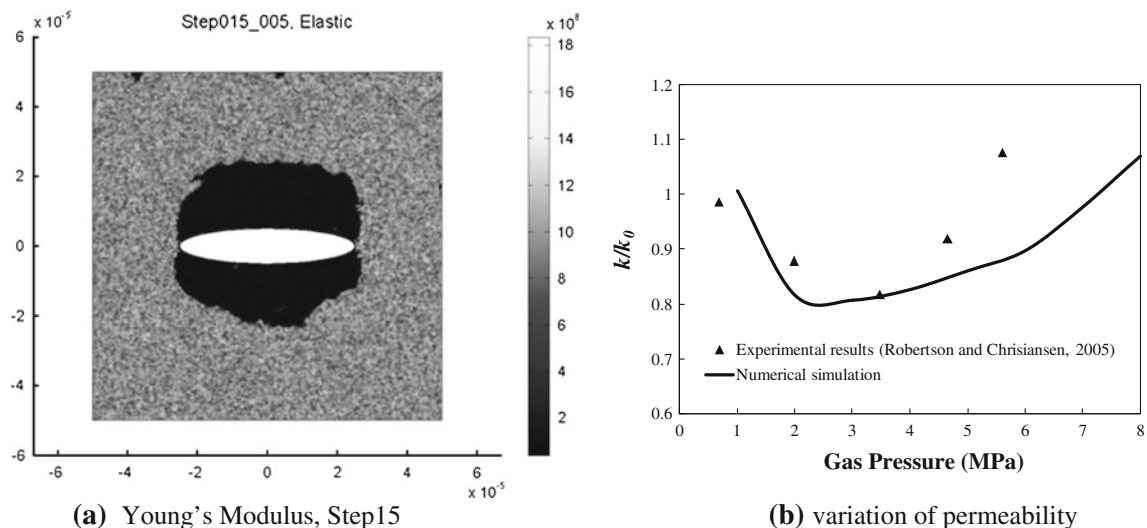
(a) Young's Modulus, Step15 **(b)** variation of permeability

Fig. 9 Comparison of the numerical results with the experimental observation (Robertson and Chrisiansen 2005) for **a** Young's modulus distribution and **b** variation of permeability

controls the evolutions of both coal matrix damage and coal permeability under the influence of gas adsorption. In this respect, the Langmuir swelling coefficient and coal heterogeneity are also very important factors affecting the coal matrix swelling/shrinking.

References

Biot MA (1941) General theory of three-dimensional consolidation. J Appl Phys 12:155–164

Bustin M (2002) Research activities on CO_2, H_2S, and SO_2 sequestration at UBC, Coal-Seq I Forum, Houston Texas, 14–15 March

COMSOL AB (2008) COMSOL Multiphysics version 3.5, user's guide and reference guide. http:\\www.comsol.com

Connell LD, Lu M, Pan ZJ (2010) An analytical coal permeability model for tri-axial strain and stress conditions. Int J Coal Geol 84:103–114

Cui XJ, Bustin RM (2005) Volumetric strain associated with methane desorption and its impact on coalbed gas production from deep coal seams. AAPG Bull 89(9):1181–1202

Cui XJ, Bustin RM, Chikatamarla L (2007) Adsorption-induced coal swelling and stress: implications for methane production and acid gas sequestration into coal seams. J Geophys Res 112(B10)

Durucan S, Ahsan M, Shi JQ (2009) Matrix shrinkage and swelling characteristics of European coals. Energy Procedia 1:3055–3062

Gray I (1987) Reservoir engineering in coal seams: part 1—the physical process of gas storage and movement in coal seams. SPE Reserv Eng 2(1):28–34

Izadi G, Wang SG, Elsworth D, Liu J, Wu Y, Pone D (2011) Permeability evolution of fluid-infiltrated coal containing discrete fractures. Int J Coal Geol 85:202–211

Karacan C (2003) An effective method for resolving spatial distribution of adsorption kinetics in heterogeneous porous media: application for carbon dioxide sequestration in coal. Chem Eng Sci 58(20):4681–4693

Karacan C (2007) Swelling-induced volumetric strains internal to a stressed coal associated with CO_2 sorption. Int J Coal Geol 72(3–4):209–220

Karacan C, Mitchell G (2003) Behavior and effect of different coal microlithotypes during gas transport for carbon dioxide sequestration into coal seams. Int J Coal Geol 53(4):201–217

Levine JR (1996) Model study of the influence of matrix shrinkage on absolute permeability of coalbed reservoirs, coalbed methane and coal geology. Geol Soc Spec Publ 109:197–212

Liu HH, Rutqvist J (2010) A new coal-permeability model: internal swelling stress and fracture–matrix interaction. Transp Porous Media 82:157–171

Liu J, Wang J, Chen Z, Wang S, Elsworth D, Jiang Y (2011) Impact of transition from local swelling to macro swelling on the evolution of coal permeability. Int J Coal Geol 88(1):31–40

Mavor MJ, Vaughn JE (1997) Increasing absolute permeability in the San Juan basin Fruitland formation. In: Proceedings of the coalbed methane symposium, University of Alabama, Tuscaloosa, Alabama

Palmer I, Mansoori J (1998) How permeability depends on stress and pore pressure in coalbeds: a new model. SPE Reserv Eval Eng 1(6):539–544

Pan ZJ, Connell LD (2007) A theoretical model for gas adsorption-induced coal swelling. Int J Coal Geol 69(3–4):243–252

Pan ZJ, Connell LD (2011) Modelling of anisotropic coal swelling and its impact on permeability behaviour for primary and enhanced coalbed methane recovery. Int J Coal Geol 85(3–4):257–267

Pan ZJ, Connell LD (2012) Modelling permeability for coal reservoirs: a review of analytical models and testing data. Int J Coal Geol 92(3–4):1–44

Patching TH (1970) Retention and release of gas in coal—a review. Can Min Metall Bull 63(703):1302–1308

Perera M, Ranjith P, Peter M (2011) Effects of saturation medium and pressure on strength parameters of Latrobe Valley brown coal: carbon dioxide, water and nitrogen saturations. Energy 36(12): 6941–6947

Ranjith P, Jasinge D, Choi S, Mehic M, Shannon B (2010) The effect of CO_2 saturation on mechanical properties of Australian black coal using acoustic emission. Fuel 89(8):2110–2117

Robertson EP (2005) Measurement and modeling of sorption-induced strain and permeability changes in coal. Prepared for the US Department of Energy through the INL LDRD Program under DOE Idaho Operations Office Contract DE-AC07-05ID14517, p 61

Robertson EP, Chrisiansen RL (2005) Modeling permeability in coal using sorption-induced strain data. In: SPE 97068, SPE annual technical conference and exhibition. Dallas, TX, USA

Seidle JP, Jeansonne MW, Erickson DJ (1992) Application of matchstick geometry to stress dependent permeability in coals. In: SPE 24361, SPE rocky mountain regional meeting. Casper, Wyoming

Viete DR, Ranjith P (2006) The effect of CO_2 on the geomechanical and permeability behaviour of brown coal: implications for coal seam CO_2 sequestration. Int J Coal Geol 66(3):204–216

Vinokurova EB, Ketslakh AI (1985) Influence of gas composition on the modulus of elasticity of gas-impregnated anthracites. J Min Sci 21(5):458–460

Wang S, Elsworth D, Liu J (2010) Evolution of permeability in coal to absorbing gases: a preliminary study. In: The 44th US rock mechanics symposium, Salt Lake City, UT, USA

Witherspoon PA, Wang JSY, Iwai K, Gale JE (1980) Validity of cubic law for fluid flow in a deformable rock fracture. Water Resour Res 16:1016–1024

Wu Y, Liu J, Chen Z, Elsworth D, Pone D (2011) A dual poroelastic model for CO_2-enhanced coalbed methane recovery. Int J Coal Geol 86(2–3):177–189

Zhu WC, Tang CA (2004) Micromechanical model for simulating the fracture process of rock. Rock Mech Rock Eng 37(1):25–56

Zhu WC, Wei CH, Liu J, Qu HY, Elsworth DA (2011) A model of coal–gas interaction under variable temperatures. Int J Coal Geol 86(2–3):213–221